

1 Recovery of high quality metagenome-assembled genomes  
2 from full-scale activated sludge microbial communities in a  
3 tropical climate using longitudinal metagenome sampling

4 Mindia A. S. Haryono<sup>1</sup>, Ying Yu Law<sup>2</sup>, Krithika Arumugam<sup>2</sup>, Larry C.-W.  
5 Liew<sup>2</sup>, Thi Quynh Ngoc Nguyen<sup>2</sup>, Daniela I. Drautz-Moses<sup>2</sup>, Stephan C.  
6 Schuster<sup>2</sup>, Stefan Wuertz<sup>2</sup>, and Rohan B. H. Williams<sup>1,§</sup>

7 <sup>1</sup>Singapore Centre for Environmental Life Sciences Engineering, National University of  
8 Singapore, Singapore, 117456

9 <sup>2</sup>Singapore Centre for Environmental Life Sciences Engineering, Nanyang Technological  
10 University, Singapore, 637551

11 <sup>§</sup>Corresponding author: [lsirbhw@nus.edu.sg](mailto:lsirbhw@nus.edu.sg)

12

August 22, 2021

## Abstract

Analysis of metagenome data based on the recovery of draft genomes (so called metagenome-assembled genomes, or MAG) have assumed an increasingly central role in microbiome research in recent years. Microbial communities underpinning the operation of wastewater treatment plants are particularly challenging targets for MAG analysis due to their high ecological complexity, and remain important, albeit understudied, microbial communities that play a key role in mediating interactions between human and natural ecosystems. In this paper, we consider strategies for recovery of MAG sequence from time series metagenome surveys of full-scale activated sludge microbial communities. We generate MAG catalogues from this set of data using several different strategies, including the use of multiple individual sample assemblies, two variations on multi-sample co-assembly and a recently published MAG recovery workflow using deep learning. We obtain a total of just under 9,100 draft genomes, which collapse to around 3,100 non-redundant genomic clusters. We examine the strengths and weaknesses of these approaches in relation to MAG yield and quality, showing the co-assembly offers clear advantages over single-sample assembly. Around 1000 MAGs were candidates for being considered high quality, based on single-copy marker gene occurrence statistics, however only 58 MAG formally meet the MIMAG criteria for being high quality draft genomes. These findings carry broader implications for performing genome-resolved metagenomics on highly complex communities, the design and implementation of genome recoverability strategies, MAG decontamination and the search for better binning methodology.

## Introduction

Over course of the last half decade the use of genome-resolved metagenome analysis has become a common approach for dealing with whole community metagenome data collected from microbiomes and complex microbial communities (Quince et al., 2017b). Starting with deeply sequenced genomic DNA, metagenome assembly is performed in order to reconstruct short fragments of the underlying member genomes, which are then analysed further using data clustering procedures (genome binning (Sangwan et al., 2016)) with the objective of recovering draft genomes of the member species, referred to as metagenome-assembled genomes (MAG). This approach, now readily deployable due to the availability of near-automated bioinformatics workflows (Uritskiy et al., 2018), has been successfully used on a great variety of microbial communities (Almeida et al., 2021; Nayfach et al., 2019; Parks et al., 2017; Pasolli et al., 2019; Singleton et al., 2021; Stewart et al., 2019; Tully et al., 2018) and has resulted in recovery of draft genomes for many new species that would have most likely remained uncharacterised due to a lack of knowledge of their required culture conditions (Parks et al., 2017).

Despite impressive accomplishments, the MAG approach still harbours many challenges and limitations. By nature, short read metagenome assemblies remain highly fractionated, resulting from the limited ability of short read sequencing to accurately

57 capture complex repeat regions (Chen et al., 2020) and the difficulties encountered in  
58 reconstructing sequence from closely related strains or sub-species (Bertrand et al.,  
59 2019; Quince et al., 2020; Vicedomini et al., 2021; Quince et al., 2017a). In practice a  
60 draft genome obtained from these methods would contain at best, tens and, more typ-  
61 ically, hundreds, of distinct contigs, and so there are inherent difficulties in accurately  
62 determining the degree of genome completeness and the extent of contamination from  
63 non-cognate genomes (Chen et al., 2020), and in identifying the presence of horizon-  
64 tally transferred sequence (Douglas and Langille, 2019). Another limitation relates to  
65 impact of the eco-genomic complexity of the community under study, both in terms of  
66 genomic diversity, particularly at sub-species or strain level, but also in terms of over-  
67 all community richness and evenness (Quince et al., 2017b). When applied to microbial  
68 communities of high complexity, a typical MAG analysis will return many draft genomes  
69 of unremarkable quality, as defined by currently accepted criteria (Bowers et al., 2017).

70 Some of these challenges may be addressed using emerging methods, such as long-  
71 read sequencing (Arumugam et al., 2021; Singleton et al., 2021), synthetic long-read  
72 methods (Bishara et al., 2018) and adaptations of chromosome conformation capture  
73 methods (Bickhart et al., 2021; DeMaere and Darling, 2019). However all of these new  
74 techniques are themselves complex and will contain their own limitations, and since  
75 the vast majority of non-amplicon metagenome data has been collected using Illumina  
76 shotgun sequencing, there remains a clear need to develop more refined methods to  
77 recover genomes from short read metagenome assemblies.

78 Complex microbial communities associated with full-scale wastewater treatment  
79 plants (activated sludge) are particularly challenging targets for MAG-based analyses  
80 due to high species richness, high species evenness and extent of genetic diversity (Law  
81 et al., 2016; Pérez et al., 2019; Singleton et al., 2021; Yang et al., 2020; Ye et al., 2020)  
82 . Recent comparative analyses undertaken with amplicon sequencing surveys suggest  
83 that these activated sludge communities are more complex than the host-associated  
84 microbiomes, including the human fecal microbiomes, by an order of magnitude (Wu  
85 et al., 2019). To date, several MAG-based analyses of activated sludge communities  
86 have been reported, varying in sequencing depth, raw sequence and availability of re-  
87 covered genome (MAG) sequence, including one recently published study that employed  
88 long-read metagenomics (Singleton et al., 2021). In this paper, we consider strategies  
89 for recovery of MAG sequence from time series metagenome surveys of full-scale ac-  
90 tivated sludge microbial communities. We generate MAG catalogues from this set of  
91 data using several different strategies, including the use of multiple individual sample  
92 assemblies, two variations on multi-sample co-assembly and a recently published MAG  
93 recovery workflow using deep learning (Nissen et al., 2021). We examine the strengths  
94 and weaknesses of these approaches in relation to MAG yield and quality, and present a  
95 catalogue of non-redundant draft genomes comprised of at least putatively high quality  
96 under the MIMAG criteria. All raw data and high quality MAG sequence have been  
97 made available via NCBI (BioProject Accession PRJNA731554), and key data products,  
98 including metagenome assemblies and the complete set of recovered MAG sequence data,  
99 are being made publicly available on Zenodo (DOI 10.5281/zenodo.5215738).

## 100 Results

### 101 Summary of data obtained and overall study design

102 As part of a long-term sampling project surveying the microbial ecology of wastewater  
103 treatment in tropical climates, we sampled activated sludge from aerobic-stage tanks in  
104 a full-scale wastewater treatment plant in Singapore, known to perform enhanced bio-  
105 logical phosphorus removal (EBPR) and previously studied by us in Law et al. (2016),  
106 obtaining 24 samples over approximately a 10 month period. The median sampling in-  
107 terval was 7 days (mean 13 days, with range 7-56 days). At each sampling event, we  
108 obtained samples for DNA extraction from the aerobic treatment tank (including a panel  
109 of co-assayed physico-chemical measurements), and performed whole community shot-  
110 gun metagenome sequencing on all samples. In total, we obtained 1.5 billion reads with  
111 a mean of 62.6M reads per sample (range: 45.7M–101.4M; **Supplementary Table 1**).  
112 From these data we constructed catalogues of metagenome-assembled genomes (MAG)  
113 using several approaches as described below.

114 In our primary analysis, we performed both individual sample assembly of data from  
115 each of the 24 samples and co-assembly of the same ensemble of data (see **Methods:**  
116 **Genome-resolved metagenome analysis**), in order to formally compare the results  
117 of each of these two major approaches to MAG-based analysis. Metagenome assembly  
118 was performed using metaSPAdes (Nurk et al., 2017) and genome binning was performed  
119 using MetaBAT2 (Kang et al., 2019) in both cases. From the co-assembly, we generated  
120 two sets of MAGs, one using coverage profiles generated across all 24 samples and the  
121 other generated using the entire read set treated as a single meta-sample (see **Methods:**  
122 **Genome-resolved metagenome analysis**), which we refer to as multi-BAM and  
123 single-BAM co-assembly binning, respectively.

124 As a secondary analysis, we performed metagenome binning using a recently pub-  
125 lished deep learning workflow called VAMB (Nissen et al., 2021), which is described later  
126 in the article.

Assembly–binning procedure	Total	Putative genome quality			
		High	Medium	Low	Unclassified
Individual assemblies ( $n=24$ )	3429	341 (9.9%)	934 (27.2%)	1775 (51.8%)	379 (11.1%)
Co-assembly, single–BAM	1997	285 (14.3%)	589 (29.5%)	878 (44.0%)	245 (12.3%)
Co-assembly, multi–BAM	1712	303 (17.7%)	532 (31.1%)	641 (37.4%)	236 (13.8%)
VAMB	1941	156 (8.0%)	475 (24.5%)	1293 (66.6%)	17 (0.9%)

Table 1: Number of MAGs (percentage of the total observed within workflow) from different assembly–binning workflows categorised by initial quality evaluation. Percentage of total MAG number per workflow in brackets.

## 127 Comparative analysis of individual sample assembly and co-assembly 128 from MetaBAT2–based workflows

129 A total of 7,138 MAGS were recovered from the three types of assembly–binning work-  
130 flows. Between 94 and 273 MAGs (mean 143) were obtained from each individual sample  
131 assembly, with a total of 3,429 MAGs being generated from all 24 individual assemblies  
132 (**Table 1** and **Supplementary Table 2**). Approximately 10% and 27% of individ-  
133 ual sample assembly MAGs were candidates for being high (pHQ) and medium qual-  
134 ity (MQ) under the MIMAG criteria (Bowers et al., 2017) (see **Methods: Genome**  
135 **quality estimates**). The single–BAM and multi–BAM co-assembly binning workflows  
136 returned 1,997 and 1,712 MAGs, respectively (**Table 1**). The proportions of pHQ– and  
137 MQ–MAGs obtained from co-assemblies were higher compared to those observed from  
138 the ensemble of individual sample assemblies (**Table 1**), with 14.3% and 17.7% being  
139 classifiable as pHQ–MAGs in the single–BAM and multi–BAM co-assembly binning,  
140 respectively, and approximately 30% of MAG from each type of co-assembly binning  
141 workflow, holding MQ status.

142 The proportion of reads mapped to co-assemblies was higher (mean 92%;  $n=2$ ) than  
143 the proportion observed to map to individual sample assemblies (mean 67%,  $n=24$ )  
144 (**Supplementary Table 2**).

145 As expected, estimated MAG genome quality demonstrated a strong association  
146 with relative abundance–expressed as a normalised coverage measure that permits com-  
147 parisons across workflows whose variable number of input sequence reads would bias  
148 estimation (see **Methods: Genome–resolved metagenome analysis**)–with the pro-  
149 portion of pHQ MAGs being highest in the top 10%–ile of the normalised coverage,  
150 and decreasing in a roughly uniform manner thereafter (**Fig. 1**). A similar trend was  
151 observed for MQ–MAGs, and the proportion of poor quality MAGs expanded in the  
152 bottom 50% of the normalised coverage distribution.

153 Given the expected high degree of genomic redundancy among the complete set  
154 of 7,138 MAGs generated from the three assembly–binning workflows employed, the  
155 entire set was de-replicated and grouped into non-redundant genome clusters (*secondary*  
156 *clusters* as defined by the dRep workflow (Olm et al., 2017); see **Methods: Genome**  
157 **de–replication procedures**). In total 2,912 non–redundant clusters were obtained,  
158 comprised of between 1 and 26 MAGs (median 2; mean 2.45) (**Supplementary Table**

159 **3**). Of these 2,912 secondary clusters, 382 (13.1%) contained at least one MAG that  
160 was pHQ, and 690 (23.7%) contained MAGs that were MQ at best, with the remainder  
161 containing MAGs of either low quality (LQ;  $n = 1576$ ; 54.1%) or else unclassifiable (UC;  
162  $n = 264$ ; 9.1%).

163 To gain further insight into the effectiveness and inter-relationship of each type of  
164 genome recovery workflow, the set of 2,912 non-redundant clusters were further cate-  
165 gorised according to the the types of workflow which had contributed at least one genome  
166 to a given non-redundant cluster (**Supplementary Table 4** and **Fig. 2A**). Of these  
167 2912 secondary clusters, 346 (11.9%) contained genomes contributed from both indi-  
168 vidual sample assemblies and both types of co-assembly binning procedure, and 1070  
169 (36.8%) contained MAGs recovered from type of co-assembly but not any individual  
170 sample assembly (**Fig. 2A**). Relatively few MAGs were observed arising from indi-  
171 vidual sample assembly and from either, but not both, types of co-assembly (23 and 14  
172 secondary clusters, respectively, against single-BAM and multi-BAM; **Fig. 2A**). In con-  
173 trast, we observed substantial numbers of secondary clusters that were only comprised  
174 of MAGs obtained from within one of the three workflows (**Fig. 2A**).

175 We then examined how these associations were patterned by genome quality and  
176 relative abundance, using a composite quality statistic as defined in the dRep pipeline  
177 and a normalised measure of MAG coverage that adjusted for differences in coverage  
178 that are present across the three types of workflows (**Fig. 2B–2H**). Each secondary  
179 clusters was represented by the best quality MAG observed in that cluster, as defined  
180 by the maximum dRep quality score within the highest MAG quality category from that  
181 cluster.

182 We observed that the 346 secondary clusters comprised of MAGs recovered from  
183 all three workflows had the highest overall coverage and over half of these secondary  
184 clusters contained at least one pHQ genome (189/346 or 54.6%). In the larger set  
185 of 1070 secondary clusters that arose from both types of co-assembly workflow, 185  
186 (17.3%) and 483 (45.1%) of these held at least one genome of pHQ and MQ level,  
187 respectively. These secondary clusters were also distributed across a lower coverage range  
188 than the previous category (**Fig. 2G**), consistent with the expectation that co-assembly  
189 procedures can recover genomes of less common or rare taxa. Of the remaining set of  
190 1496 secondary clusters from the remaining four categories there were only 8 (0.54%)  
191 which held candidates for being pHQ-MAGs, with the remainder holding unremarkable  
192 or frankly poor quality (**Fig. 2B–2F**).

193 We then undertook several secondary analyses to examine whether co-assembly or  
194 individual sample assembly showed any inherent biases in genome quality (**Fig. 3**).  
195 Firstly, for secondary clusters that contained MAGs from all three workflows (**Fig.**  
196 **2A–2B**) we examined the proportion of pHQ-MAG in secondary cluster that came  
197 from either type of co-assembly or from an individual assembly, but observed no clear  
198 pattern in relation to the origin of pHQ-MAGS (**Fig. 3A**). Secondly, we compared  
199 completeness and contamination statistics within a subset of 48 secondary clusters that  
200 contained at least one pHQ genome sourced from co-assembly and at least one pHQ  
201 genome from an individual assembly. Removing all genomes that did not attain pHQ



202 status, on average this subset of secondary clusters contained 1.8 pHQ-MAGs (range:  
203 1–2) sourced from the co-assembly workflows and 6.3 pHQ-MAGs (range: 1–22) arising  
204 from the individual assembly workflow. We calculated median completeness and median  
205 contamination within each secondary cluster, conditioned on workflow type, observing a  
206 bias towards higher completeness (**Fig. 3B, 3D**) and a lower contamination (**Fig. 3C,**  
207 **3D**) in co-assembled genomes relative to genomes obtained from individual assemblies.

208 Collectively, these data suggest that if we focus attention on recovered genomes that  
209 are plausibly of high quality, then these results indicate, in the communities studied  
210 here, that co-assembly conveys clear advantages in regards MAG yield.

## 211 **Decontamination of recovered draft genomes**

212 To improve the number of high quality MAGs produced from the workflows above, we  
213 applied RefineM (Parks et al., 2017) to all MAGs from the three assembly procedures that  
214 possessed completeness of more than 90% (1,307 MAGs, contributed from 550 secondary  
215 clusters) regardless of their contamination and strain heterogeneity levels, as calculated  
216 by CheckM (Parks et al., 2015), considering these suitable candidates for refinement to  
217 high quality.

218 The results of the decontamination analysis are summarised in **Table 2A**. Of the  
219 1,307 MAGs, 929 (71.1%) were classified as pHQ prior to decontamination, and of these,  
220 855 (92.0%) retained the same quality level after application of RefineM. Of the remain-  
221 ing 74 pHQ-MAGs, the majority 94.6% were converted to MQ, with only four being  
222 reduced to LQ status. Of the 127 MAGs originally classified as MQ, 35.4% (45/127)  
223 attained pHQ status following application of RefineM. In the set of 251 MAGs that held  
224 UC status before decontamination, only 7.2% and 16.7% improved their quality to pHQ  
225 and MQ, respectively, suggesting that most MAGs that hold contamination above 10%  
226 are likely to be of highly flawed construction.

227 Across all MAGs, the average number of contigs removed by RefineM was 59 (range:  
228 0–3,309) with CheckM completeness, contamination, and strain heterogeneity reduced  
229 on average by 1.7%, 5.8%, and 0.5, respectively (**Supplementary Table 5**).

## 230 **Genomes recovered using a deep variational autoencoder workflow (VAMB)**

231 As a secondary, complementary analysis to the canonical approach taken above, we per-  
232 formed genome recovery using a recently described workflow called VAMB that utilises  
233 deep variational autoencoders (Nissen et al., 2021). Using data from the 24 individual-  
234 sample assemblies, VAMB generated 1,941 MAGs of minimum total sequence length of  
235 200kbp (to match that used by the default MetaBAT2-based workflows).

236 Of the recovered draft genomes, 8.0%, 24.5%, 66.6%, and 0.9% were classified as  
237 pHQ, MQ, LQ and UC, respectively (**Table 1** and **Supplementary Table 6**). The  
238 pHQ-MAGs from VAMB were strongly associated with those detected by the MetaBAT2  
239 workflows, with only 1 and 5 secondary clusters containing pHQ-MAGs (**Figure 4A**)  
240 and MQ-MAGs (**Figure 4B**), respectively, that were not recovered by any other work-  
241 flow. While a substantive number of secondary clusters containing LQ-MAGs were

recovered by VAMB (**Table 1** and **Figure 4C**), interestingly, the number of secondary clusters containing UC-MAGs was two orders of magnitude lower than the number observed in the MetaBAT2 workflows (**Figure 4D**). This suggests that the VAMB methodology may likely provide superior control of gross contamination, although possibly at the expense of recovery of more complete, higher quality MAGs.

As above, we applied RefineM workflow to the 175 MAGs with completeness above 90% (contributed from 36 distinct secondary clusters), which were primarily comprised of pHQ-MAGs ( $n = 156$ , 89.14%). After application of the RefineM workflow, 59% of pHQ-MAGs retained their quality status, and 38% were reduced to MQ-status. The numbers of MAGs in remaining categories was low (**Table 2B**). The average number of contigs removed by RefineM was 53 (range: 0-495), and completeness, contamination and strain heterogeneity were reduced on average by 4.6%, 1.4% and 1.3 units, respectively (**Supplementary Table 6**).

		After						After			
		pHQ	MQ	LQ	UC			pHQ	MQ	LQ	UC
Before	pHQ	855	70	4	0	Before	pHQ	100	54	2	0
	MQ	45	80	2	0		MQ	3	12	0	0
	UC	18	42	2	189		UC	1	1	0	2

(a) MetaBAT2 workflows

(b) VAMB workflow

Table 2: Number of MAGs categorised by genome quality assignments before and after decontamination with RefineM for (a) MAGs obtained from MetaBAT2 workflows and (b) MAGs from VAMB workflow. Input MAGs held CheckM-estimated completeness > 90%.

## Catalogue of high quality genomes from tropical climate activated sludge

The entire set of MAGs recovered from all four sources were combined into a single set of 9,079 bins (7138 bins from the MetaBAT2 workflows and 1941 from VAMB; see **Supplementary Table 7**), corresponding to 3,113 secondary clusters, as defined by dRep. Of the 9079 MAGs defined by this analysis, 1085 (11.9%) were categorised as pHQ. Of these 1044 (96.2%), 124 and 5 were comprised of less than 500, 50 and 10 contigs or less, 1066 MAGs (98.3%) held an N50 of at least 10kb and 142 MAGs (13.1%) contained at least one copy of the 5S, 16S and 23S SSU-rRNA genes. The 1085 pHQ MAGs were split among 382 different secondary clusters.

Taxonomic analysis (**Fig. 4**) showed a predominance of phyla *Bacteroidota* and *Proteobacteria*, which accounted for 44.4% (482/1085 MAGs within 100 secondary clusters) and 20.6% (223/1085 MAGs in 98 secondary clusters) of MAGs classified as pHQ. Other phyla that were observed at relative frequencies above 1% were *Chloroflexota* (5.4%, 59 MAGs within 22 secondary clusters), *Planctomycetota* (5.3%, 57 MAGs within 37 secondary clusters), *Spirochaetota* (4.4%, 48 MAGs within 7 secondary clusters), *Actinobacteriota* (3.8%, 41 MAGs within 19 secondary clusters), *Acidobacteriota* (2.7%, 29



271 MAGs within 17 secondary clusters), *Myxococcota* (2.3%, 25 MAGs within 17 secondary  
272 clusters), *Nitrospirota* (2.3%, 25 MAGs within 4 secondary clusters), *Bdellovibrionota*  
273 (2.7%, 29 MAGs within 18 secondary clusters) and *Verrucomicrobiota* (2.3%, 25 MAGs  
274 within 16 secondary clusters).

275 Across the 382 secondary clusters, only 14 (3.7%) were comprised of MAGs anno-  
276 tated to species level and 155 (40.6%) were annotated to genus level, highlighting that  
277 over half the recovered pHQ MAGs were likely to be previously uncharacterised. Species-  
278 level annotations were observed for the polyphosphate accumulating organisms (PAO)  
279 *Candidatus Accumulibacter SK-02* ( $n = 2$  MAGs) (Skenner et al., 2015) and the  
280 cyanobacteria *Obscuribacter phosphatis* (Soo et al., 2014; Stokholm-Bjerregaard et al.,  
281 2017) ( $n = 2$  MAGs), and the glycogen accumulating organism, *Candidatus Competibac-*  
282 *ter* (McIlroy et al., 2014) ( $n = 1$  MAG). Interestingly, we recovered a single MAG  
283 from *Romboutsia timonensis*, a member of the human gut microbiome (Ricaboni et al.,  
284 2016), and to our knowledge not previously identified in activated sludge communities,  
285 and genomes of the methane-oxidising bacteria *Methylosarcina fibrata* (Hamilton et al.,  
286 2015) ( $n = 2$  MAG). Genomes from the denitrifier *Hyphomicrobium denitrificans* (Mar-  
287 tineau et al., 2014) were recovered ( $n = 2$  MAG), along with genomes from two species  
288 within the UBA2359 lineage within order *Chitinophagales* (GTDB), namely *Sphingobac-*  
289 *teriales* bacterium TSM.CSS and *Sphingobacteriales* bacterium TSM.CSM and genomes  
290 from recently identified novel lineages in phyla *Bacteroidetes*, *Chloroflexi* and *Chlorobi*  
291 (see **Supplementary Table 8** for full details of species-level identifications).

292 The ammonia-oxidising bacteria (AOB), *Nitrosomonas* (Kowalchuk and Stephen,  
293 2001) ( $n = 16$  MAG), and the nitrite oxidising bacteria (NOB), *Nitrospira* (Vijayan et al.,  
294 2021) ( $n = 25$  MAG), both key functional species in activated sludge-mediated biopro-  
295 cesses, were only represented at genus level.

296 When we applied the more stringent form of the MIMAG criteria for high quality  
297 genomes (Bowers et al., 2017), that is, those with at least 18 tRNAs and the presence of  
298 a complete set of rRNA genes, only 58 HQ-MAGs were identified. In addition, 6 more  
299 high quality MAGs were recovered from RefineM pipeline, resulting in a total 64 high  
300 quality MAGs submitted to NCBI.

## 301 Comparison to other MAG catalogues recovered from activated sludge

302 We systematically compared our MAG catalogue to several others that have been re-  
303 cently obtained (Singleton et al., 2021; Ye et al., 2020), using genome de-replication (see  
304 Methods: Genome de-replication procedures) and same criteria recently used in a com-  
305 parative analysis of MAG catalogues from multiple cow rumen microbiomes (Watson,  
306 2021). Collectively, this analysis defined a total of 6,328 secondary clusters, containing  
307 on average 1.9 MAGs (median 1.0; range 1–54 MAG). We examined the membership of  
308 these secondary clusters in relation to catalogue of origin (**Fig. 5**). Only 7 secondary  
309 clusters contained genomes from all three source catalogues. A larger proportion of re-  
310 lated genomes ( $n = 314$ ) was observed between our catalogue and that of Ye et al. (2020),  
311 than between our study and the catalogue of Singleton et al. (2021), which may reflect  
312 the more diverse geographies and mixture of operational regimes incorporated in the

313 former study. We highlight however, that our analysis is retrospective and thus should  
314 be interpreted with caution.

## 315 Discussion

316 In this paper we undertake a comprehensive genome-resolved metagenome survey of  
317 an activated sludge microbial community from a full-scale, tropical climate wastewater  
318 treatment plant, based on a time-series survey design. We obtain a total of just under  
319 9,100 draft genomes, which collapse to around 3,100 non-redundant genomic clusters  
320 (defined under a stringent degree of relatedness). Around 1000 MAGs were candidates  
321 for being considered high quality, based on single-copy marker statistics (referred to pHQ  
322 in our analysis) but 58 MAGs formally meet the MIMAG criteria for being high quality  
323 draft genomes. In building these MAG catalogues, we undertake a systematic compar-  
324 ison of MAG recovery strategies, based on the use of individual-sample assemblies and  
325 two variations on the use of co-assemblies (using the combination of metaSPAdes for  
326 performing assemblies and MetaBAT2 for genome recovery). Additionally, we compared  
327 these results to those obtained from the use of a recently released deep learning vari-  
328 ational autoencoder called VAMB (Nissen et al., 2021), which appears to convey some  
329 advantages in relation to control of MAG contamination. As discussed below, these  
330 findings carry broader implications for conducting genome-resolved metagenomics on  
331 highly complex communities.

332 The genomes recovered at pHQ level in this study represented 11 phyla, captured at a  
333 relative frequency of above 1%, with just under half being members of *Bacteriodota* and  
334 *Proteobacteria*, and represent the most comprehensive catalogue obtained from tropical  
335 climate activated sludge communities, building on our previous efforts (Arumugam et al.,  
336 2019, 2021; Law et al., 2016; Qiu et al., 2020). Wastewater microbial communities from  
337 tropical climates are understudied relative to their temperate climate counterparts, as  
338 are the bioprocesses that they support. Given the urgent need to understand the impact  
339 of climate change at microbial scales of life (Cavicchioli et al., 2019), such communities  
340 will become an increasingly important target of study, given their role as mediators of  
341 the interface between human and natural ecosystems (McLellan et al., 2015). In the  
342 present case, we obtained pHQ or confirmed HQ MAGs for expected taxa conveying key  
343 functionality to activated sludge bioprocesses including the AOB *Nitrosomonas*, NOB  
344 *Nitrospira*, the PAO *Candidatus Accumulibacter* and the GAO *Candidatus Competibac-*  
345 *ter*. Notable unexpected findings included, but were not limited to, the cyanobacterial  
346 PAO species *Obscuribacter phosphatis* and *Romboutsia timonensis*, previously identified  
347 in the human gut and plausibly an immigrant species from that source.

348 The large proportion of recovered genomes that hold unremarkable quality is ex-  
349 pected, given the recognised challenges of performing these analysis on highly complex  
350 microbial communities (Pasoli et al., 2019) and the known complexity of full-scale ac-  
351 tivated sludge microbial communities, which are estimated to be more complex than  
352 the human gut microbiome by around an order of magnitude (Wu et al., 2019). The  
353 complexity of the community in regards to taxonomic novelty is also seen in the fact

354 that around 60% of the recovered pHQ hold no assignment at species or genus level, and  
355 by the relatively low degree of recapitulation of genomes from other activated sludge  
356 catalogues. Consistent with the recognised limitations of MAG analyses conducted from  
357 short-read sequence data, the recovered genomes are unlikely to be resolved to strain  
358 level, and the size and complexity of the dataset limited the use of a recent genome-bin  
359 workflow for strain deconvolution (Quince et al., 2020) (data not shown). Nonethe-  
360 less, the kind of densely sampled longitudinal data collected here is ideally suited for  
361 developing such strain-aware genome recovery methods.

362 As part of this analysis, we have undertaken a comprehensive comparison of indi-  
363 vidual sample assembly and co-assembly approaches for genome recovery, which has  
364 been relatively unexplored in the literature to date. Current thinking on MAG analysis  
365 suggests that assembling data from individual samples will aid the recovery of higher  
366 quality, relatively abundant genomes, while co-assembly will assist in the recovery of  
367 lower abundance genomes with the trade-off of artefacts associated with multi-sample  
368 analysis (Hofmeyr et al., 2020; Pasolli et al., 2019), including cross-sample chimeras  
369 (Chen et al., 2020), split-bins (Arumugam et al., 2021) and increased probability of  
370 recovering pan-genomic level (Chen et al., 2020), although this will no doubt be de-  
371 pendent on, the nature of the co-assembled samples (longitudinal versus cross-sectional;  
372 (Pasolli et al., 2019)), sample replication number, genetic diversity, community complex-  
373 ity and, of course, sequencing depth. In their comparative analysis on co-assembly and  
374 individual assembly of infant and maternal gut microbiomes, Pasolli *et al.* found little  
375 difference in number or quality of recovered genomes from either method, which included  
376 an analysis of both longitudinal and cross-sectional sampling designs, concluding that  
377 application to longer time-series would likely result in higher MAG yields (Pasolli et al.,  
378 2019). The findings of the present study are consistent with that view, with substan-  
379 tially higher numbers of pHQ-level MAGs being recovered from co-assembly procedures.  
380 We find some clear indications that co-assembly is advantageous in regards to genome  
381 quality, and, at least in the subset of MAGs that are recovered at pHQ level by both  
382 approaches, there is clear evidence that co-assembly will provide cognate MAGs with  
383 higher completeness and lower contamination statistics, as defined by single copy marker  
384 gene analysis: the extent to which this is generalisable to other settings is unclear.

385 Unexpectedly, we find the two specific modes of co-assembly are each capable of high  
386 MAG yields suggesting that greater depth *per se*, as implemented in the single-BAM  
387 approach, will recover almost as many pHQ MAGs (285 versus 303; **Table 1**) as the  
388 canonical differential coverage approach (multi-BAM). Additionally, the computational  
389 overheads of co-assembly can be substantial, as seen in the present case, and which  
390 may be untenable or impractical in some settings. Obviously this would also influence  
391 the choice of metagenome assembler, for example, MEGAHIT may be a more suitable  
392 choice of assembler than metaSPAdes for datasets at, or above, the scale of data employed  
393 here. Interestingly, as applied to this dataset, the deep-learning based VAMB workflow  
394 recovered pHQ MAGs that largely recapitulated those from the MetaBAT2 workflows.  
395 Collectively, these findings reinforce the view that MAG recovery is highly context-  
396 specific in relation to the community under study (Vollmers et al., 2017).

397 There remains an urgent need for methods to identify non-cognate contigs in frac-  
398 tionated assemblies, with the impact of contamination on gene-level becoming more  
399 widely recognised (Arkhipova, 2020), and one recently published analysis suggests that  
400 up to 15–30% of publicly-available MAGs classified at pHQ level will harbour chimeric  
401 content (Orakov et al., 2021). In the present study, we have examined removal of possible  
402 contamination using the RefineM workflow (Parks et al., 2017). Our results shed light  
403 on the strengths and weaknesses of the different recovery workflows we employed. From  
404 the MetaBAT2 workflows, there was a high degree of robustness in the case of recovered  
405 genomes that were classified at pHQ level, with over 90% retaining their pHQ status  
406 upon the application of RefineM. In the case of draft genomes that held high levels of  
407 contamination upon a backbone of high completeness, most also remained within the  
408 same genome quality category following de-contamination, suggesting that these recov-  
409 ered sequence constructions are fundamentally flawed. In the case of the bins recovered  
410 from VAMB, while around one third of pHQ changed quality level to MQ, there was an  
411 under-representation of complete genomes initially showing high degrees of contamina-  
412 tion, suggesting that VAMB may be quite robust to the formation of chimeras. Whether  
413 this is a general property, or a consequence of the high redundant nature of time-series  
414 data, is a subject for further study.

415 Collectively, our results reinforce the ongoing need for analysis procedures suitable for  
416 recovering high quality MAGs from metagenome data, also highlighted by recent calls for  
417 more careful manual curation of recovered genomes (Chen et al., 2020; Lui et al., 2021)  
418 and the use of complementary sequencing, including long read (Arumugam et al., 2021;  
419 Singleton et al., 2021), synthetic long read (Bishara et al., 2018) and chromosome con-  
420 firmation capture methods (Bickhart et al., 2021; DeMaere and Darling, 2019). Another  
421 relevant development is the direct use of assembly graphs in MAG recovery, including  
422 for the recovery of strain level sequence (Brown et al., 2020; Mallawaarachchi et al.,  
423 2020; Quince et al., 2020). Further attention could also be placed on the use of alter-  
424 native feature representations for contig sequence and/or coverage data: most methods  
425 developed to date have used Euclidean space (of various dimensionality, ranging from  
426 two to several hundred), but other representations may hold substantive advantages, for  
427 example hyperspherical or hyperbolic embeddings (Ding and Regev, 2021) or related  
428 manifold learning methods *e.g.* as implicit in the use of VAMB (Nissen et al., 2021).

## 429 **Methods**

### 430 **Metagenome extraction and sequencing**

431 The field sampling methodology, sample handling, DNA extraction and sequencing meth-  
432 ods have been previously described by us (Law et al., 2016). At a full-scale operational  
433 wastewater treatment plant in Singapore, treating mostly waste of domestic origin, we  
434 sampled the aerobic stage of an activated sludge tank known to perform enhanced biolog-  
435 ical phosphate removal (EBPR). At each sampling event, we obtained multiple samples  
436 for DNA extraction from the aerobic treatment tank and collected a panel of relevant

437 physico-chemical measurements (data not analysed in this paper). Samples were snap  
438 frozen in a liquid nitrogen dry shipper immediately upon retrieval from the tank, and  
439 transported to the laboratory for subsequent genomic DNA extraction and sequencing on  
440 Illumina HiSeq2500 using a read length of 251bp (paired end) (see (Law et al., 2016) for  
441 details of all gDNA extraction, library preparation and sequencing protocols).

#### 442 **Genome-resolved metagenome analysis**

443 Unless otherwise stated data analysis was performed in the R Statistical Computing  
444 Environment (version 4.0.5) (R Core Team, 2021).

#### 445 **Initial data processing**

446 The raw FASTQ files were processed using cutadapt (version 1.5, with default arguments  
447 except `--overlap 10 -m 30 -q 20`) (Martin, 2011).

#### 448 **Genome recovery from individual sample assemblies**

449 From the processed read data, we initially performed individual sample assemblies using  
450 SPAdes (Nurk et al., 2017) in `-meta` mode with maximum  $k$ -mer value of 127, and per-  
451 formed metagenome binning using MetaBAT2 version 2.12.1 (default settings) to obtain  
452 an initial set of MAGs from each sample. Coverage for each contigs were extracted from  
453 SPAdes  $k$ -mer coverage, converted to log scale, and averaged per bin. To compare esti-  
454 mates of MAG coverage between samples, we normalised MAG coverages by centering  
455 using the per-sample mean per-MAG coverage, scaling by the per-sample standard de-  
456 viation of coverage and then placing back on a positive scale by subtracting the smallest  
457 normalised coverage value across the entire set of MAGs.

#### 458 **Genome recovery from co-assemblies**

459 Processed read data from the 24 samples were co-assembled with SPAdes-3.13.0 (Nurk  
460 et al., 2017) (default parameters except `--meta -m 2900 -k 21,33,55,77,99,127 -t`  
461 `50`). Binning was performed on contigs over 2500 bp in length with MetaBAT2 (Kang  
462 et al., 2019) (version 2.12.1 with default parameters except `-d -t 40 -m 2500 -v`),  
463 employing two different approaches, namely: 1) using contigs from the co-assembly and  
464 24 sorted .bam files made by aligning reads from each of the 24 datasets to the contigs  
465 from co-assembly, referred to as the *multi-BAM co-assembly* and 2) using contigs from  
466 the co-assembly and a single sorted bam file made by aligning all reads from the 24  
467 datasets to the contigs from co-assembly (referred to as a *single-BAM co-assembly*).

#### 468 **Genome recovery using deep variational autoencoder (VAMB)**

469 The recently published metagenome binner VAMB was employed on the 24 individual  
470 sample assemblies, following the described procedure in (Nissen et al., 2021). Briefly,  
471 all assembled contigs with minimum length of 2.500bp were compiled into a FASTA



472 catalogue (`-m 2500 --nozip`). Processed read data from each of the 24 samples were  
473 mapped to this catalogue using Bowtie2 (version 2.3.4.3) (Langmead and Salzberg, 2012)  
474 and Samtools (version 1.9) (Li et al., 2009), with read depth being calculated using the  
475 MetaBAT2 script `jgi_summarize_bam_contig_depths`; default settings). We then ran  
476 VAMB (version 3.0.2) on the catalogue and read depth data using default parameters  
477 except for minimum total sequence length set at 200kb (`-o C` as the sample separator  
478 and `--minfasta 200000`).

## 479 Genome quality estimates

480 Genome quality estimation of all all bins obtained from all four different pipelines  
481 (individual sample assemblies, single-BAM co-assembly, multi-BAM co-assembly and  
482 VAMB) was performed by running the CheckM (version 1.0.13) (Parks et al., 2015)  
483 `lineage_wf` workflow using default parameters (except `-t 20 -x fa` or `-t 20 -x fna`  
484 for VAMB bins). The output was then tabulated with the CheckM `qa` command using  
485 20 threads (`-t 20`). MAG quality was then classified using the MIMAG criteria (Bowers  
486 et al., 2017) with modifications as follows: 1) MAGs with CheckM completeness ( $C_p$ ) and  
487 CheckM contamination ( $C_n$ ) values  $>90$  and  $<5$ , respectively, were classified as candi-  
488 dates for being high quality (pHQ) genomes bins; 2) MAGs with  $C_p \geq 50$  and  $C_n < 10$   
489 were categorized as being of putatively medium quality (MQ) ; 3) MAGs with  $C_p < 50$   
490 and  $C_n < 10$  were classified as candidate low quality (LQ) and 4) MAGs that did not  
491 fall into any of the above three categories were unclassified (UC). The N50 value ( $N_{50}$ )  
492 for each MAG was calculated using QUAST version 5.0.0 (Gurevich et al., 2013) with  
493 flags `--mgm --rna-finding --min-contig 1 --max-ref-number 0`. for each MAG,  
494 we computed an overall (univariate) quality statistic,  $Q_d$  as defined by within the dRep  
495 workflow (Olm et al., 2017), defined as  $Q_d = C_p - 5C_n + \frac{C_n S_h}{100} + 0.5 \log N_{50}$ . MAGs  
496 defined as pHQ under the MIMAG criteria were further screened for the presence of tR-  
497 NAs (minimum of 18) and a complete rRNA operon (defined as the presence of at least  
498 one copy of each of the 5S, 16S and 23S SSU-rRNA genes, irrespective of whether they  
499 were harboured on a single contig or not), and if present were denoted as *high quality*  
500 (HQ) MAGs.

## 501 Genome de-replication procedures

502 We identified putative sets of cognate genomes using the dRep (version 2.2.3) (Olm et al.,  
503 2017) `compare` workflow executed with default settings with 20 threads (`-p 20`). Four  
504 dereplication analyses were performed; 1) dereplication of the complete set of MAGs ; 2)  
505 de-replication of the set of 9079 MAGs combining those identified in 1) with the addi-  
506 tional MAGs recovered from using VAMB (**Supplementary Table 7**); 3) de-replication  
507 of the set of 142 HQ MAGs from our analyses combined with the set of 3139 MAGs  
508 available from previously published MAG analyses of activated sludge communities (see  
509 below) and 4) The entire set of MAGs from 2) combined with the 3139 MAGs from  
510 references in dRep `compare` workflow with the same parameters (`-p 80 --S_algorithm`



511 `fastANI --multiround_primary_clustering -sa 0.95 -nc 0.3`) as used in a compa-  
512 rable recent de-replication analysis of rumen MAG catalogues (Watson, 2021).

### 513 **Taxonomic and functional annotation of recovered genomes**

514 Taxonomic classification of the collective set of 9079 MAG sequences was performed using  
515 the GTDB-Tk (version 0.3.2) (Chaumeil et al., 2019) `classify_wf` workflow with default  
516 settings (`-x fa --cpus 30`). Prediction of tRNA and rRNA were made using Prokka  
517 (version 1.14.6) (Seemann, 2014) executed with default parameters. Predicted rRNA  
518 genes were aligned to the SILVA database (version 138.1; release dates 12/06/2020 and  
519 30/06/2020) (Quast et al., 2013) using SINA (version 1.7.1) (Pruesse et al., 2012) with  
520 settings `-S --search-min-sim 0.95 -t -v --meta-fmt csv --lca-fields tax_slv,`  
521 `tax_embl, tax_ltp, tax_gg, tax_rdp.`

### 522 **MAG refinement**

523 We performed decontamination of MAG sequences using RefineM (version 0.0.24) (Parks  
524 et al., 2017). Briefly, tetranucleotide signature and coverage profiles for contigs were  
525 calculated using `scaffold_stats` workflow. Contigs with divergent genomic properties  
526 were identified with outliers (default settings) and removed using the `filter_bins` work-  
527 flow. Genes were predicted using the `call_genes` workflow and annotated with DIA-  
528 MOND (Buchfink et al., 2015) against the `gtdb_r95_protein_db.2020-07-30.dmond` and  
529 `gtdb_r95_taxonomy.2020-07-30.tsv` databases, within the `taxon_profile` workflow.  
530 Contigs with divergent taxonomic assignments were then identified with `taxon_filter`  
531 and removed with `filter_bins`. After decontamination, genome quality was reanalysed  
532 using CheckM, as described above, and bins reclassified if indicated.

### 533 **Publicly available MAG catalogues**

534 We obtained the following MAG sequence data from the following published studies: 1)  
535 a set of 1083 MAGs based on long read metagenome data obtained from 23 wastewater  
536 treatment plants in Denmark (Singleton et al., 2021); 2) a set of 2045 MAGs recovered  
537 from meta-analysis of Ye et al. (2020), which includes WWTP samples from several  
538 locations in China (data collected by the authors of (Ye et al., 2020)), Singapore (data  
539 from (Law et al., 2016)), Denmark (data from (Munck et al., 2015)), USA (data from  
540 (Chu et al., 2018)), Argentina (data from (Ibarbalz et al., 2016)), Slovenia (data from  
541 (McIlroy et al., 2016)) and Switzerland (data from (Ju et al., 2019)); 3) one MAG  
542 sequence available from NCBI submitted from the time-series metagenome survey of a  
543 full-scale activated sludge community in Argentina (Buenos Aires) (Pérez et al., 2019);  
544 and 4) ten MAG sequences available from NCBI from the metagenome survey of three  
545 conventional WWTPs in Taiwan inoculated with exogenous anammox pellets (Yang  
546 et al., 2020). We re-estimated the genome quality of all MAGs using the CheckM based  
547 approach described above.

## 548 **Data visualisation**

549 We constructed unrooted phylograms from MAG sequence data using GTDB-Tk (ver-  
550 sion 0.3.2) based on bacterial single-copy gene sets (bac120\_ms gene sets) and imported  
551 the `.tree` file into R using the `read.tree` function from `ggtree` package (version 2.4.2)  
552 (Yu et al., 2017) and subsequently rendered using the `ggtree` function. Venn diagrams  
553 were constructed using the R package `VennDiagram` (version 1.6.0) (Chen and Boutros,  
554 2011).

## 555 **Author Contribution Statement**

556 The study was designed by Y.Y.L, S.W. and R.B.H.W. Y.Y.L and R.B.H.W designed  
557 field sampling procedures, which was conducted by L.C.W.L and led by Y.Y.L. L.C.W.L  
558 and T.Q.N.N performed gDNA extractions. D.I.D-M and S.C.S advised on gDNA ex-  
559 traction procedures and protocols and generated short read sequencing data. M.A.S.H,  
560 K.A. and R.B.H.W designed and performed data analysis. All authors contributed to  
561 data interpretation. The manuscript was primarily written by R.B.H.W and M.A.S.H  
562 with specific sections contributed by other authors.

## 563 **Acknowledgements**

564 This research was supported by the Singapore National Research Foundation and Min-  
565 istry of Education under the Research Centre of Excellence Programme and by program  
566 grants 1102-IRIS-10-02 (S.W., R.B.H.W and S.C.S) from the National Research Foun-  
567 dation (NRF). The computational work was performed in part on resources of the Na-  
568 tional Supercomputing Centre (NSCC, Singapore) supported by Project 11000984. We  
569 thank our numerous colleagues from the Public Utilities Board (Republic of Singapore)  
570 for access to facilities and biomass which permitted this work to be undertaken.

## 571 **Description of Supplementary Materials**

### 572 **Supplementary Table 1**

573 Summary of sequencing read data from each of the 24 samples analysed in this study.

574

### 575 **Supplementary Table 2**

576 Assembly and binning statistics of each of the 24 individual assemblies and the two co-  
577 assemblies (constructed with SPAdes and MetaBAT2)

578

### 579 **Supplementary Table 3**

580 Summary statistics for the 2,912 secondary (non-redundant) clusters from MAGs recov-  
581 ered by 24 individual assemblies and two co-assemblies (constructed with SPAdes and  
582 MetaBAT2)

583

584 **Supplementary Table 4**

585 Summary data for all 7,138 MAGs recovered from 24 individual assemblies and two co-  
586 assemblies (constructed with SPAdes and MetaBAT2)

587

588 **Supplementary Table 5**

589 MAGs from 24 individual assemblies and two co-assemblies that possessed completeness  
590 of more than 90%

591

592 **Supplementary Table 6**

593 Summary data for the MAGs recovered from VAMB workflow

594

595 **Supplementary Table 7**

596 Secondary (non-redundant) clusters of the complete set of MAGs recovered from all four  
597 different workflows (24 individual assemblies, two co-assemblies, and VAMB)

598

599 **Supplementary Table 8**

600 Putative high quality (pHQ) MAGs recovered from all four different workflows

601

602

603 **References**

604 A. Almeida, S. Nayfach, M. Boland, F. Strozzi, M. Beracochea, Z. J. Shi, K. S. Pollard,  
605 E. Sakharova, D. H. Parks, P. Hugenholtz, N. Segata, N. C. Kyrpides, and R. D.  
606 Finn. A unified catalog of 204,938 reference genomes from the human gut microbiome.  
607 *Nature Biotechnology*, 39(1):105–114, 2021. ISSN 1546-1696. doi: 10.1038/s41587-020-  
608 0603-3. URL <https://doi.org/10.1038/s41587-020-0603-3>.

609 I. R. Arkhipova. Metagenome proteins and database contamination. *mSphere*, 5(6), Nov  
610 2020. ISSN 2379-5042 (Electronic); 2379-5042 (Linking). doi: 10.1128/mSphere.00854-  
611 20.

612 K. Arumugam, C. Bağcı, I. Bessarab, S. Beier, B. Buchfink, A. Górska, G. Qiu, D. H.  
613 Huson, and R. B. H. Williams. Annotated bacterial chromosomes from frame-shift-  
614 corrected long-read metagenomic data. *Microbiome*, 7(1):61, Apr 2019. ISSN 2049-  
615 2618 (Electronic); 2049-2618 (Linking). doi: 10.1186/s40168-019-0665-y.

616 K. Arumugam, I. Bessarab, M. A. S. Haryono, X. Liu, R. E. Zuniga-Montanez, S. Roy,  
617 G. Qiu, D. I. Drautz-Moses, Y. Y. Law, S. Wuertz, F. M. Lauro, D. H. Huson, and  
618 R. B. H. Williams. Recovery of complete genomes and non-chromosomal replicons  
619 from activated sludge enrichment microbial communities with long read metagenome  
620 sequencing. *npj Biofilms and Microbiomes*, 7(1):23, 2021. doi: 10.1038/s41522-021-  
621 00196-6. URL <https://doi.org/10.1038/s41522-021-00196-6>.

- 622 D. Bertrand, J. Shaw, M. Kalathiyappan, A. H. Q. Ng, M. S. Kumar, C. Li, M. Dvornicic,  
623 J. P. Soldo, J. Y. Koh, C. Tong, O. T. Ng, T. Barkham, B. Young, K. Marimuthu,  
624 K. R. Chng, M. Sikic, and N. Nagarajan. Hybrid metagenomic assembly enables  
625 high-resolution analysis of resistance determinants and mobile elements in human  
626 microbiomes. *Nature Biotechnology*, 37(8):937–944, 2019. doi: 10.1038/s41587-019-  
627 0191-2. URL <https://doi.org/10.1038/s41587-019-0191-2>.
- 628 D. M. Bickhart, M. Kolmogorov, E. Tseng, D. M. Portik, A. Korobeynikov, I. Tol-  
629 stoganov, G. Uritskiy, I. Liachko, S. T. Sullivan, S. B. Shin, A. Zorea, V. P.  
630 Andreu, K. Panke-Buisse, M. H. Medema, I. Mizrahi, P. A. Pevzner, and T. P.  
631 Smith. Generation of lineage-resolved complete metagenome-assembled genomes  
632 by precision phasing. *bioRxiv*, 2021. doi: 10.1101/2021.05.04.442591. URL  
633 <https://www.biorxiv.org/content/early/2021/05/04/2021.05.04.442591>.
- 634 A. Bishara, E. L. Moss, M. Kolmogorov, A. E. Parada, Z. Weng, A. Sidow, A. E.  
635 Dekas, S. Batzoglou, and A. S. Bhatt. High-quality genome sequences of uncultured  
636 microbes by assembly of read clouds. *Nature Biotechnology*, 36(11):1067–1075, 2018.  
637 doi: 10.1038/nbt.4266. URL <https://doi.org/10.1038/nbt.4266>.
- 638 R. M. Bowers, N. C. Kyrpides, R. Stepanauskas, M. Harmon-Smith, D. Doud, T. B. K.  
639 Reddy, F. Schulz, J. Jarett, A. R. Rivers, E. A. Eloe-Fadrosh, S. G. Tringe, N. N.  
640 Ivanova, A. Copeland, A. Clum, E. D. Becraft, R. R. Malmstrom, B. Birren, M. Po-  
641 dar, P. Bork, G. M. Weinstock, G. M. Garrity, J. A. Dodsworth, S. Yooseph, G. Sutton,  
642 F. O. Glöckner, J. A. Gilbert, W. C. Nelson, S. J. Hallam, S. P. Jungbluth, T. J. G.  
643 Ettema, S. Tighe, K. T. Konstantinidis, W.-T. Liu, B. J. Baker, T. Rattei, J. A.  
644 Eisen, B. Hedlund, K. D. McMahon, N. Fierer, R. Knight, R. Finn, G. Cochrane,  
645 I. Karsch-Mizrachi, G. W. Tyson, C. Rinke, N. C. Kyrpides, L. Schriml, G. M. Gar-  
646 rity, P. Hugenholtz, G. Sutton, P. Yilmaz, F. Meyer, F. O. Glöckner, J. A. Gilbert,  
647 R. Knight, R. Finn, G. Cochrane, I. Karsch-Mizrachi, A. Lapidus, F. Meyer, P. Yilmaz,  
648 D. H. Parks, A. Murat Eren, L. Schriml, J. F. Banfield, P. Hugenholtz, T. Woyke,  
649 and T. G. S. Consortium. Minimum information about a single amplified genome  
650 (misag) and a metagenome-assembled genome (mimag) of bacteria and archaea. *Na-  
651 ture Biotechnology*, 35(8):725–731, 2017. ISSN 1546-1696. doi: 10.1038/nbt.3893.  
652 URL <https://doi.org/10.1038/nbt.3893>.
- 653 C. T. Brown, D. Moritz, M. P. O’Brien, F. Reidl, T. Reiter, and B. D. Sullivan. Exploring  
654 neighborhoods in large metagenome assembly graphs using spacegraphcats reveals  
655 hidden sequence diversity. *Genome Biology*, 21(1):164, 2020. doi: 10.1186/s13059-  
656 020-02066-4. URL <https://doi.org/10.1186/s13059-020-02066-4>.
- 657 B. Buchfink, C. Xie, and D. H. Huson. Fast and sensitive protein alignment using  
658 diamond. *Nat Methods*, 12(1):59–60, Jan 2015. ISSN 1548-7105 (Electronic); 1548-  
659 7091 (Linking). doi: 10.1038/nmeth.3176.
- 660 R. Cavicchioli, W. J. Ripple, K. N. Timmis, F. Azam, L. R. Bakken, M. Baylis, M. J.  
661 Behrenfeld, A. Boetius, P. W. Boyd, A. T. Classen, T. W. Crowther, R. Danovaro,

- 662 C. M. Foreman, J. Huisman, D. A. Hutchins, J. K. Jansson, D. M. Karl, B. Koskella,  
663 D. B. Mark Welch, J. B. H. Martiny, M. A. Moran, V. J. Orphan, D. S. Reay, J. V.  
664 Remais, V. I. Rich, B. K. Singh, L. Y. Stein, F. J. Stewart, M. B. Sullivan, M. J. H.  
665 van Oppen, S. C. Weaver, E. A. Webb, and N. S. Webster. Scientists' warning to  
666 humanity: microorganisms and climate change. *Nat Rev Microbiol*, 17(9):569–586,  
667 Sep 2019. ISSN 1740-1534 (Electronic); 1740-1526 (Print); 1740-1526 (Linking). doi:  
668 10.1038/s41579-019-0222-5.
- 669 P.-A. Chaumeil, A. J. Mussig, P. Hugenholtz, and D. H. Parks. Gtdb-tk: a toolkit to  
670 classify genomes with the genome taxonomy database. *Bioinformatics*, 36(6):1925–  
671 1927, Nov 2019. ISSN 1367-4811 (Electronic); 1367-4803 (Print); 1367-4803 (Linking).  
672 doi: 10.1093/bioinformatics/btz848.
- 673 H. Chen and P. C. Boutros. Venndiagram: a package for the generation of highly-  
674 customizable venn and euler diagrams in r. *BMC Bioinformatics*, 12(1):35, 2011. doi:  
675 10.1186/1471-2105-12-35. URL <https://doi.org/10.1186/1471-2105-12-35>.
- 676 L.-X. Chen, K. Anantharaman, A. Shaiber, A. M. Eren, and J. F. Ban-  
677 field. Accurate and complete genomes from metagenomes. *Genome*  
678 *Research*, 30(3):315–333, 2020. doi: 10.1101/gr.258640.119. URL  
679 <http://genome.cshlp.org/content/30/3/315.abstract>.
- 680 B. T. T. Chu, M. L. Petrovich, A. Chaudhary, D. Wright, B. Murphy, G. Wells, and  
681 R. Poretsky. Metagenomics reveals the impact of wastewater treatment plants on  
682 the dispersal of microorganisms and genes in aquatic sediments. *Applied and Envi-*  
683 *ronmental Microbiology*, 84(5), 2018. ISSN 0099-2240. doi: 10.1128/AEM.02168-17.  
684 URL <https://aem.asm.org/content/84/5/e02168-17>.
- 685 M. Z. DeMaere and A. E. Darling. bin3c: exploiting hi-c sequencing data to accu-  
686 rately resolve metagenome-assembled genomes. *Genome Biology*, 20(1):46, 2019. doi:  
687 10.1186/s13059-019-1643-1. URL <https://doi.org/10.1186/s13059-019-1643-1>.
- 688 J. Ding and A. Regev. Deep generative model embedding of single-cell rna-seq profiles  
689 on hyperspheres and hyperbolic spaces. *Nat Commun*, 12(1):2554, May 2021. ISSN  
690 2041-1723 (Electronic); 2041-1723 (Linking). doi: 10.1038/s41467-021-22851-4.
- 691 G. M. Douglas and M. G. I. Langille. Current and Promising Approaches to Iden-  
692 tify Horizontal Gene Transfer Events in Metagenomes. *Genome Biology and Evolu-*  
693 *tion*, 11(10):2750–2766, 08 2019. ISSN 1759-6653. doi: 10.1093/gbe/evz184. URL  
694 <https://doi.org/10.1093/gbe/evz184>.
- 695 A. Gurevich, V. Saveliev, N. Vyahhi, and G. Tesler. Quast: quality assessment tool for  
696 genome assemblies. *Bioinformatics*, 29(8):1072–1075, Apr 2013. ISSN 1367-4811 (Elec-  
697 tronic); 1367-4803 (Print); 1367-4803 (Linking). doi: 10.1093/bioinformatics/btt086.
- 698 R. Hamilton, K. D. Kits, V. A. Ramonovskaya, O. N. Rozova, H. Yurimoto, H. Iguchi,  
699 V. N. Khmelenina, Y. Sakai, P. F. Dunfield, M. G. Klotz, C. Knief, H. J. M. Op den

- 700 Camp, M. S. M. Jetten, F. Bringel, S. Vuilleumier, M. M. Svenning, N. Shapiro,  
701 T. Woyke, Y. A. Trotsenko, L. Y. Stein, and M. G. Kalyuzhnaya. Draft genomes of  
702 gammaproteobacterial methanotrophs isolated from terrestrial ecosystems. *Genome*  
703 *Announc*, 3(3), Jun 2015. ISSN 2169-8287 (Print); 2169-8287 (Electronic). doi:  
704 10.1128/genomeA.00515-15.
- 705 S. Hofmeyr, R. Egan, E. Georganas, A. C. Copeland, R. Riley, A. Clum, E. Eloe-  
706 Fadrosh, S. Roux, E. Goltsman, A. Buluç, D. Rokhsar, L. Olikier, and K. Yelick.  
707 Terabase-scale metagenome coassembly with metahipmer. *Scientific Reports*, 10  
708 (1):10689, 2020. ISSN 2045-2322. doi: 10.1038/s41598-020-67416-5. URL  
709 <https://doi.org/10.1038/s41598-020-67416-5>.
- 710 F. M. Ibarbalz, E. Orellana, E. L. M. Figuerola, and L. Erijman. Shotgun  
711 metagenomic profiles have a high capacity to discriminate samples of activated  
712 sludge according to wastewater type. *Applied and Environmental Microbiology*,  
713 82(17):5186–5196, 2016. ISSN 0099-2240. doi: 10.1128/AEM.00916-16. URL  
714 <https://aem.asm.org/content/82/17/5186>.
- 715 F. Ju, K. Beck, X. Yin, A. Maccagnan, C. S. McArdell, H. P. Singer, D. R. Johnson,  
716 T. Zhang, and H. Bürgmann. Wastewater treatment plant resistomes are shaped  
717 by bacterial composition, genetic exchange, and upregulated expression in the efflu-  
718 ent microbiomes. *The ISME Journal*, 13(2):346–360, 2019. ISSN 1751-7370. doi:  
719 10.1038/s41396-018-0277-8. URL <https://doi.org/10.1038/s41396-018-0277-8>.
- 720 D. D. Kang, F. Li, E. Kirton, A. Thomas, R. Egan, H. An, and Z. Wang. Metabat  
721 2: an adaptive binning algorithm for robust and efficient genome reconstruction from  
722 metagenome assemblies. *PeerJ*, 7:e7359, 2019. ISSN 2167-8359 (Print); 2167-8359  
723 (Electronic); 2167-8359 (Linking). doi: 10.7717/peerj.7359.
- 724 G. A. Kowalchuk and J. R. Stephen. Ammonia-oxidizing bacteria: a model for molecular  
725 microbial ecology. *Annu Rev Microbiol*, 55:485–529, 2001. ISSN 0066-4227 (Print);  
726 0066-4227 (Linking). doi: 10.1146/annurev.micro.55.1.485.
- 727 B. Langmead and S. L. Salzberg. Fast gapped-read alignment with bowtie 2. *Nat*  
728 *Methods*, 9(4):357–359, Mar 2012. ISSN 1548-7105 (Electronic); 1548-7091 (Print);  
729 1548-7091 (Linking). doi: 10.1038/nmeth.1923.
- 730 Y. Law, R. H. Kirkegaard, A. A. Cokro, X. Liu, K. Arumugam, C. Xie, M. Stokholm-  
731 Bjerregaard, D. I. Drautz-Moses, P. H. Nielsen, S. Wuertz, and R. B. H. Williams.  
732 Integrative microbial community analysis reveals full-scale enhanced biological phos-  
733 phorus removal under tropical conditions. *Scientific Reports*, 6(1):25719, 2016. ISSN  
734 2045-2322. doi: 10.1038/srep25719. URL <https://doi.org/10.1038/srep25719>.
- 735 H. Li, B. Handsaker, A. Wysoker, T. Fennell, J. Ruan, N. Homer, G. Marth, G. Abecasis,  
736 and R. Durbin. The sequence alignment/map format and samtools. *Bioinformatics*, 25  
737 (16):2078–2079, Aug 2009. ISSN 1367-4811 (Electronic); 1367-4803 (Print); 1367-4803  
738 (Linking). doi: 10.1093/bioinformatics/btp352.



- 739 L. M. Lui, T. N. Nielsen, and A. P. Arkin. A method for achieving complete microbial  
740 genomes and improving bins from metagenomics data. *PLoS Comput Biol*, 17(5):  
741 e1008972, May 2021. ISSN 1553-7358 (Electronic); 1553-734X (Print); 1553-734X  
742 (Linking). doi: 10.1371/journal.pcbi.1008972.
- 743 V. Mallawaarachchi, A. Wickramarachchi, and Y. Lin. GraphBin: refined bin-  
744 ning of metagenomic contigs using assembly graphs. *Bioinformatics*, 36(11):3307–  
745 3313, 03 2020. ISSN 1367-4803. doi: 10.1093/bioinformatics/btaa180. URL  
746 <https://doi.org/10.1093/bioinformatics/btaa180>.
- 747 M. Martin. Cutadapt removes adapter sequences from high-throughput sequencing reads.  
748 *EMBnet.journal*, 17(1):10–12, 2011. ISSN 2226-6089. doi: 10.14806/ej.17.1.200. URL  
749 <http://journal.embnet.org/index.php/embnetjournal/article/view/200>.
- 750 C. Martineau, C. Villeneuve, F. Mauffrey, and R. Villemur. Complete genome sequence  
751 of hyphomicrobium nitratorans strain nl23, a denitrifying bacterium isolated from  
752 biofilm of a methanol-fed denitrification system treating seawater at the montreal  
753 biodome. *Genome Announc*, 2(1), Jan 2014. ISSN 2169-8287 (Print); 2169-8287  
754 (Electronic). doi: 10.1128/genomeA.01165-13.
- 755 S. J. McIlroy, M. Albertsen, E. K. Andresen, A. M. Saunders, R. Kris-  
756 tiansen, M. Stokholm-Bjerregaard, K. L. Nielsen, and P. H. Nielsen. 'candida-  
757 tus competibacter'-lineage genomes retrieved from metagenomes reveal functional  
758 metabolic diversity. *ISME J*, 8(3):613–624, Mar 2014. ISSN 1751-7370 (Electronic);  
759 1751-7362 (Print); 1751-7362 (Linking). doi: 10.1038/ismej.2013.162.
- 760 S. J. McIlroy, S. M. Karst, M. Nierychlo, M. S. Dueholm, M. Albertsen, R. H. Kirkegaard,  
761 R. J. Seviour, and P. H. Nielsen. Genomic and in situ investigations of the novel un-  
762 cultured chloroflexi associated with 0092 morphotype filamentous bulking in activated  
763 sludge. *The ISME Journal*, 10(9):2223–2234, 2016. ISSN 1751-7370. doi: 10.1038/is-  
764 mej.2016.14. URL <https://doi.org/10.1038/ismej.2016.14>.
- 765 S. L. McLellan, J. C. Fisher, and R. J. Newton. The microbiome of urban waters. *Int*  
766 *Microbiol*, 18(3):141–149, Sep 2015. ISSN 1139-6709 (Print); 1139-6709 (Linking). doi:  
767 10.2436/20.1501.01.244.
- 768 C. Munck, M. Albertsen, A. Telke, M. Ellabaan, P. H. Nielsen, and M. O. A. Som-  
769 mer. Limited dissemination of the wastewater treatment plant core resistome. *Nature*  
770 *Communications*, 6(1):8452, 2015. ISSN 2041-1723. doi: 10.1038/ncomms9452. URL  
771 <https://doi.org/10.1038/ncomms9452>.
- 772 S. Nayfach, Z. J. Shi, R. Seshadri, K. S. Pollard, and N. C. Kyrpides. New in-  
773 sights from uncultivated genomes of the global human gut microbiome. *Nature*,  
774 568(7753):505–510, 2019. ISSN 1476-4687. doi: 10.1038/s41586-019-1058-x. URL  
775 <https://doi.org/10.1038/s41586-019-1058-x>.

- 776 J. N. Nissen, J. Johansen, R. L. Allesøe, C. K. Sønderby, J. J. A. Armenteros, C. H.  
777 Grønbech, L. J. Jensen, H. B. Nielsen, T. N. Petersen, O. Winther, and S. Rasmussen.  
778 Improved metagenome binning and assembly using deep variational autoencoders.  
779 *Nature Biotechnology*, 2021. ISSN 1546-1696. doi: 10.1038/s41587-020-00777-4. URL  
780 <https://doi.org/10.1038/s41587-020-00777-4>.
- 781 S. Nurk, D. Meleshko, A. Korobeynikov, and P. A. Pevzner. metaspades: a new versatile  
782 metagenomic assembler. *Genome Res*, 27(5):824–834, May 2017. ISSN 1549-5469  
783 (Electronic); 1088-9051 (Print); 1088-9051 (Linking). doi: 10.1101/gr.213959.116.
- 784 M. R. Olm, C. T. Brown, B. Brooks, and J. F. Banfield. drep: a tool for fast and accu-  
785 rate genomic comparisons that enables improved genome recovery from metagenomes  
786 through de-replication. *ISME J*, 11(12):2864–2868, Dec 2017. ISSN 1751-7370 (Elec-  
787 tronic); 1751-7362 (Print); 1751-7362 (Linking). doi: 10.1038/ismej.2017.126.
- 788 A. Orakov, A. Fullam, L. P. Coelho, S. Khedkar, D. Szklarczyk, D. R. Mende, T. S. B.  
789 Schmidt, and P. Bork. Gunc: detection of chimerism and contamination in prokaryotic  
790 genomes. *Genome Biol*, 22(1):178, Jun 2021. ISSN 1474-760X (Electronic); 1474-7596  
791 (Print); 1474-7596 (Linking). doi: 10.1186/s13059-021-02393-0.
- 792 D. H. Parks, M. Imelfort, C. T. Skennerton, P. Hugenholtz, and G. W. Tyson. CheckM:  
793 assessing the quality of microbial genomes recovered from isolates, single cells, and  
794 metagenomes. *Genome Research*, 25:1043–55, 2015.
- 795 D. H. Parks, C. Rinke, M. Chuvochina, P.-A. Chaumeil, B. J. Woodcroft, P. N.  
796 Evans, P. Hugenholtz, and G. W. Tyson. Recovery of nearly 8,000 metagenome-  
797 assembled genomes substantially expands the tree of life. *Nature Microbiology*, 2  
798 (11):1533–1542, 2017. ISSN 2058-5276. doi: 10.1038/s41564-017-0012-7. URL  
799 <https://doi.org/10.1038/s41564-017-0012-7>.
- 800 E. Pasolli, F. Asnicar, S. Manara, M. Zolfo, N. Karcher, F. Armanini, F. Begh-  
801 ini, P. Manghi, A. Tett, P. Ghensi, M. C. Collado, B. L. Rice, C. DuLong,  
802 X. C. Morgan, C. D. Golden, C. Quince, C. Huttenhower, and N. Segata. Ex-  
803 tensive unexplored human microbiome diversity revealed by over 150,000 genomes  
804 from metagenomes spanning age, geography, and lifestyle. *Cell*, 176(3):649–662.e20,  
805 2019. ISSN 0092-8674. doi: <https://doi.org/10.1016/j.cell.2019.01.001>. URL  
806 <https://www.sciencedirect.com/science/article/pii/S0092867419300017>.
- 807 M. V. Pérez, L. D. Guerrero, E. Orellana, E. L. Figuerola, L. Erij-  
808 man, and J. McGrath. Time series genome-centric analysis unveils bac-  
809 terial response to operational disturbance in activated sludge. *mSys-*  
810 *tems*, 4(4):e00169–19, Aug. 2019. doi: 10.1128/mSystems.00169-19. URL  
811 <http://msystems.asm.org/content/4/4/e00169-19.abstract>.
- 812 E. Pruesse, J. Peplies, and F. O. Glöckner. SINA: Accurate high-throughput mul-  
813 tiple sequence alignment of ribosomal RNA genes. *Bioinformatics*, 28(14):1823–

- 814 1829, 05 2012. ISSN 1367-4803. doi: 10.1093/bioinformatics/bts252. URL  
815 <https://doi.org/10.1093/bioinformatics/bts252>.
- 816 G. Qiu, X. Liu, N. M. M. T. Saw, Y. Law, R. Zuniga-Montanez, S. S. Thi, T. Q.  
817 Ngoc Nguyen, P. H. Nielsen, R. B. H. Williams, and S. Wuertz. Metabolic traits  
818 of candidatus accumulibacter clade iif strain scelse-1 using amino acids as carbon  
819 sources for enhanced biological phosphorus removal. *Environ Sci Technol*, 54(4):  
820 2448–2458, Feb 2020. ISSN 1520-5851 (Electronic); 0013-936X (Linking). doi:  
821 10.1021/acs.est.9b02901.
- 822 C. Quast, E. Pruesse, P. Yilmaz, J. Gerken, T. Schweer, P. Yarza, J. Peplies, and  
823 F. O. Glöckner. The silva ribosomal rna gene database project: improved data pro-  
824 cessing and web-based tools. *Nucleic Acids Res*, 41(Database issue):D590–6, Jan  
825 2013. ISSN 1362-4962 (Electronic); 0305-1048 (Print); 0305-1048 (Linking). doi:  
826 10.1093/nar/gks1219.
- 827 C. Quince, T. O. Delmont, S. Raguideau, J. Alneberg, A. E. Darling, G. Collins, and  
828 A. M. Eren. Desman: a new tool for de novo extraction of strains from metagenomes.  
829 *Genome iology*, 18:181, Sep 2017a.
- 830 C. Quince, A. W. Walker, J. T. Simpson, N. J. Loman, and N. Segata. Shotgun metage-  
831 nomics, from sampling to analysis. *Nature Biotechnology*, 35(9):833–844, 2017b. doi:  
832 10.1038/nbt.3935. URL <https://doi.org/10.1038/nbt.3935>.
- 833 C. Quince, S. Nurk, S. Raguideau, R. James, O. S. Soyer, J. K. Summers, A. Li-  
834 masset, A. M. Eren, R. Chikhi, and A. E. Darling. Metagenomics strain resolu-  
835 tion on assembly graphs. *bioRxiv*, 2020. doi: 10.1101/2020.09.06.284828. URL  
836 <https://www.biorxiv.org/content/early/2020/09/07/2020.09.06.284828>.
- 837 R Core Team. *R: A Language and Environment for Statistical Computing*. R Foundation  
838 for Statistical Computing, Vienna, Austria, 2021. URL <https://www.R-project.org>.
- 839 D. Ricaboni, M. Mailhe, S. Khelaifia, D. Raoult, and M. Million. Romboutsia timo-  
840 nensis, a new species isolated from human gut. *New Microbes New Infect*, 12:6–7,  
841 Jul 2016. ISSN 2052-2975 (Print); 2052-2975 (Electronic); 2052-2975 (Linking). doi:  
842 10.1016/j.nmni.2016.04.001.
- 843 N. Sangwan, F. Xia, and J. A. Gilbert. Recovering complete and draft population  
844 genomes from metagenome datasets. *Microbiome*, 4(1):8, 2016. doi: 10.1186/s40168-  
845 016-0154-5. URL <https://doi.org/10.1186/s40168-016-0154-5>.
- 846 T. Seemann. Prokka: rapid prokaryotic genome annotation. *Bioinformatics*, 30  
847 (14):2068–2069, Jul 2014. ISSN 1367-4811 (Electronic); 1367-4803 (Linking). doi:  
848 10.1093/bioinformatics/btu153.
- 849 C. M. Singleton, F. Petriglieri, J. M. Kristensen, R. H. Kirkegaard, T. Y. Michaelsen,  
850 M. H. Andersen, Z. Kondrotaitė, S. M. Karst, M. S. Dueholm, P. H. Nielsen, and M. Al-  
851 bertsen. Connecting structure to function with the recovery of over 1000 high-quality

- 852 metagenome-assembled genomes from activated sludge using long-read sequencing.  
853 *Nature Communications*, 12(1):2009, 2021. ISSN 2041-1723. doi: 10.1038/s41467-  
854 021-22203-2. URL <https://doi.org/10.1038/s41467-021-22203-2>.
- 855 C. T. Skennerton, J. J. Barr, F. R. Slater, P. L. Bond, and G. W. Tyson. Expanding  
856 our view of genomic diversity in candidatus accumulibacter clades. *Environ Microbiol*,  
857 17(5):1574–1585, May 2015. ISSN 1462-2920 (Electronic); 1462-2912 (Linking). doi:  
858 10.1111/1462-2920.12582.
- 859 R. M. Soo, C. T. Skennerton, Y. Sekiguchi, M. Imelfort, S. J. Paech, P. G. Dennis,  
860 J. A. Steen, D. H. Parks, G. W. Tyson, and P. Hugenholtz. An expanded genomic  
861 representation of the phylum cyanobacteria. *Genome Biol Evol*, 6(5):1031–1045, May  
862 2014. ISSN 1759-6653 (Electronic); 1759-6653 (Linking). doi: 10.1093/gbe/evu073.
- 863 R. D. Stewart, M. D. Auffret, A. Warr, A. W. Walker, R. Roehe, and M. Watson.  
864 Compendium of 4,941 rumen metagenome-assembled genomes for rumen microbiome  
865 biology and enzyme discovery. *Nature Biotechnology*, 37(8):953–961, 2019. doi:  
866 10.1038/s41587-019-0202-3. URL <https://doi.org/10.1038/s41587-019-0202-3>.
- 867 M. Stokholm-Bjerregaard, S. J. McIlroy, M. Nierychlo, S. M. Karst, M. Albertsen, and  
868 P. H. Nielsen. A critical assessment of the microorganisms proposed to be important  
869 to enhanced biological phosphorus removal in full-scale wastewater treatment systems.  
870 *Front Microbiol*, 8:718, 2017. ISSN 1664-302X (Print); 1664-302X (Electronic); 1664-  
871 302X (Linking). doi: 10.3389/fmicb.2017.00718.
- 872 B. J. Tully, E. D. Graham, and J. F. Heidelberg. The reconstruction of  
873 2,631 draft metagenome-assembled genomes from the global oceans. *Sci-*  
874 *entific Data*, 5(1):170203, 2018. doi: 10.1038/sdata.2017.203. URL  
875 <https://doi.org/10.1038/sdata.2017.203>.
- 876 G. V. Uritskiy, J. DiRuggiero, and J. Taylor. Metawrap – a flexible pipeline for genome-  
877 resolved metagenomic data analysis. *Microbiome*, 6(1):158, 2018. doi: 10.1186/s40168-  
878 018-0541-1. URL <https://doi.org/10.1186/s40168-018-0541-1>.
- 879 R. Vicedomini, C. Quince, A. E. Darling, and R. Chikhi. Auto-  
880 mated strain separation in low-complexity metagenomes using long  
881 reads. *bioRxiv*, 2021. doi: 10.1101/2021.02.24.429166. URL  
882 <https://www.biorxiv.org/content/early/2021/05/10/2021.02.24.429166>.
- 883 A. Vijayan, R. K. Vattiringal Jayadrathan, D. Pillai, P. Prasannan Geetha, V. Joseph,  
884 and B. S. Isaac Sarojini. Nitrospira as versatile nitrifiers: Taxonomy, ecophysiol-  
885 ogy, genome characteristics, growth, and metabolic diversity. *Journal of Basic Mi-*  
886 *crobiology*, 61(2):88–109, 2021. doi: <https://doi.org/10.1002/jobm.202000485>. URL  
887 <https://onlinelibrary.wiley.com/doi/abs/10.1002/jobm.202000485>.
- 888 J. Vollmers, S. Wiegand, and A.-K. Kaster. Comparing and evaluating metagenome  
889 assembly tools from a microbiologist’s perspective - not only size matters! *PLoS*

890 *One*, 12(1):e0169662, 2017. ISSN 1932-6203 (Electronic); 1932-6203 (Linking). doi:  
891 10.1371/journal.pone.0169662.

892 M. Watson. New insights from 33,813 publicly available metagenome-  
893 assembled-genomes (mags) assembled from the rumen micro-  
894 biome. *bioRxiv*, 2021. doi: 10.1101/2021.04.02.438222. URL  
895 <https://www.biorxiv.org/content/early/2021/04/02/2021.04.02.438222>.

896 L. Wu, D. Ning, B. Zhang, Y. Li, P. Zhang, X. Shan, Q. Zhang, M. R. Brown, Z. Li,  
897 J. D. Van Nostrand, F. Ling, N. Xiao, Y. Zhang, J. Vierheilig, G. F. Wells, Y. Yang,  
898 Y. Deng, Q. Tu, A. Wang, D. Acevedo, M. Agullo-Barcelo, P. J. J. Alvarez, L. Alvarez-  
899 Cohen, G. L. Andersen, J. C. de Araujo, K. F. Boehnke, P. Bond, C. B. Bott, P. Bovio,  
900 R. K. Brewster, F. Bux, A. Cabezas, L. Cabrol, S. Chen, C. S. Criddle, C. Etchebe-  
901 here, A. Ford, D. Frigon, J. Sanabria, J. S. Griffin, A. Z. Gu, M. Habagil, L. Hale,  
902 S. D. Hardeman, M. Harmon, H. Horn, Z. Hu, S. Jauffur, D. R. Johnson, J. Keller,  
903 A. Keucken, S. Kumari, C. D. Leal, L. A. Lebrun, J. Lee, M. Lee, Z. M. P. Lee, M. Li,  
904 X. Li, Y. Liu, R. G. Luthy, L. C. Mendonça-Hagler, F. G. R. de Menezes, A. J. Mey-  
905 ers, A. Mohebbi, P. H. Nielsen, A. Oehmen, A. Palmer, P. Parameswaran, J. Park,  
906 D. Patsch, V. Reginatto, F. L. de los Reyes, B. E. Rittmann, A. Noyola, S. Ros-  
907 setti, J. Sidhu, W. T. Sloan, K. Smith, O. V. de Sousa, D. A. Stahl, K. Stephens,  
908 R. Tian, J. M. Tiedje, N. B. Tooker, J. D. Van Nostrand, D. De los Cobos Vas-  
909 concelos, M. Wagner, S. Wakelin, B. Wang, J. E. Weaver, G. F. Wells, S. West,  
910 P. Wilmes, S.-G. Woo, J.-H. Wu, L. Wu, C. Xi, M. Xu, T. Yan, M. Yang, M. Young,  
911 H. Yue, T. Zhang, Q. Zhang, W. Zhang, Y. Zhang, H. Zhou, J. Zhou, X. Wen, T. P.  
912 Curtis, Q. He, Z. He, P. H. Nielsen, P. J. J. Alvarez, C. S. Criddle, J. M. Tiedje,  
913 T. P. Curtis, D. A. Stahl, B. E. Rittmann, and G. W. M. Consortium. Global di-  
914 versity and biogeography of bacterial communities in wastewater treatment plants.  
915 *Nature Microbiology*, 4(7):1183–1195, 2019. doi: 10.1038/s41564-019-0426-5. URL  
916 <https://doi.org/10.1038/s41564-019-0426-5>.

917 Y. Yang, J. Pan, Z. Zhou, J. Wu, Y. Liu, J.-G. Lin, Y. Hong, X. Li, M. Li,  
918 and J.-D. Gu. Complex microbial nitrogen-cycling networks in three dis-  
919 tinct anammox-inoculated wastewater treatment systems. *Water Research*, 168:  
920 115142, 2020. ISSN 0043-1354. doi: 10.1016/j.watres.2019.115142. URL  
921 <https://www.sciencedirect.com/science/article/pii/S0043135419309169>.

922 L. Ye, R. Mei, W.-T. Liu, H. Ren, and X.-X. Zhang. Machine learning-aided analyses  
923 of thousands of draft genomes reveal specific features of activated sludge processes.  
924 *Microbiome*, 8(1):16, 2020. ISSN 2049-2618. doi: 10.1186/s40168-020-0794-3. URL  
925 <https://doi.org/10.1186/s40168-020-0794-3>.

926 G. Yu, D. K. Smith, H. Zhu, Y. Guan, and T. T.-Y. Lam. ggtree: an r  
927 package for visualization and annotation of phylogenetic trees with their  
928 covariates and other associated data. *Methods in Ecology and Evolution*,  
929 8(1):28–36, 2017. doi: <https://doi.org/10.1111/2041-210X.12628>. URL  
930 <https://besjournals.onlinelibrary.wiley.com/doi/abs/10.1111/2041-210X.12628>.

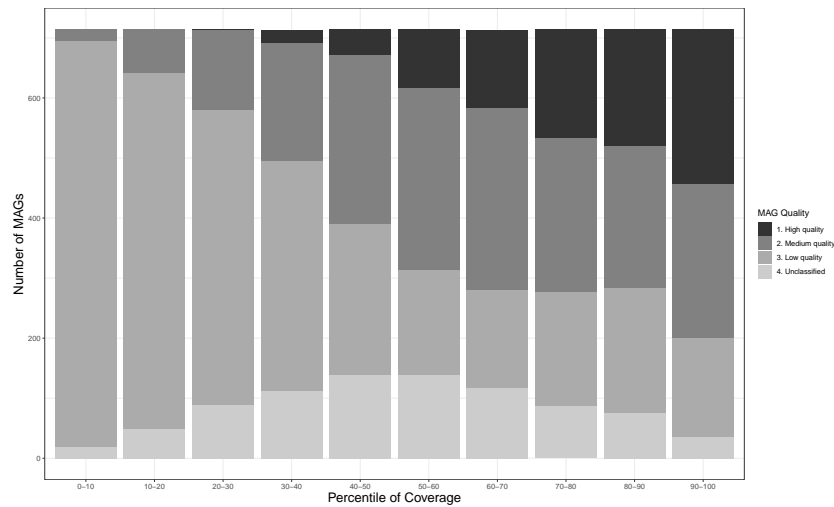
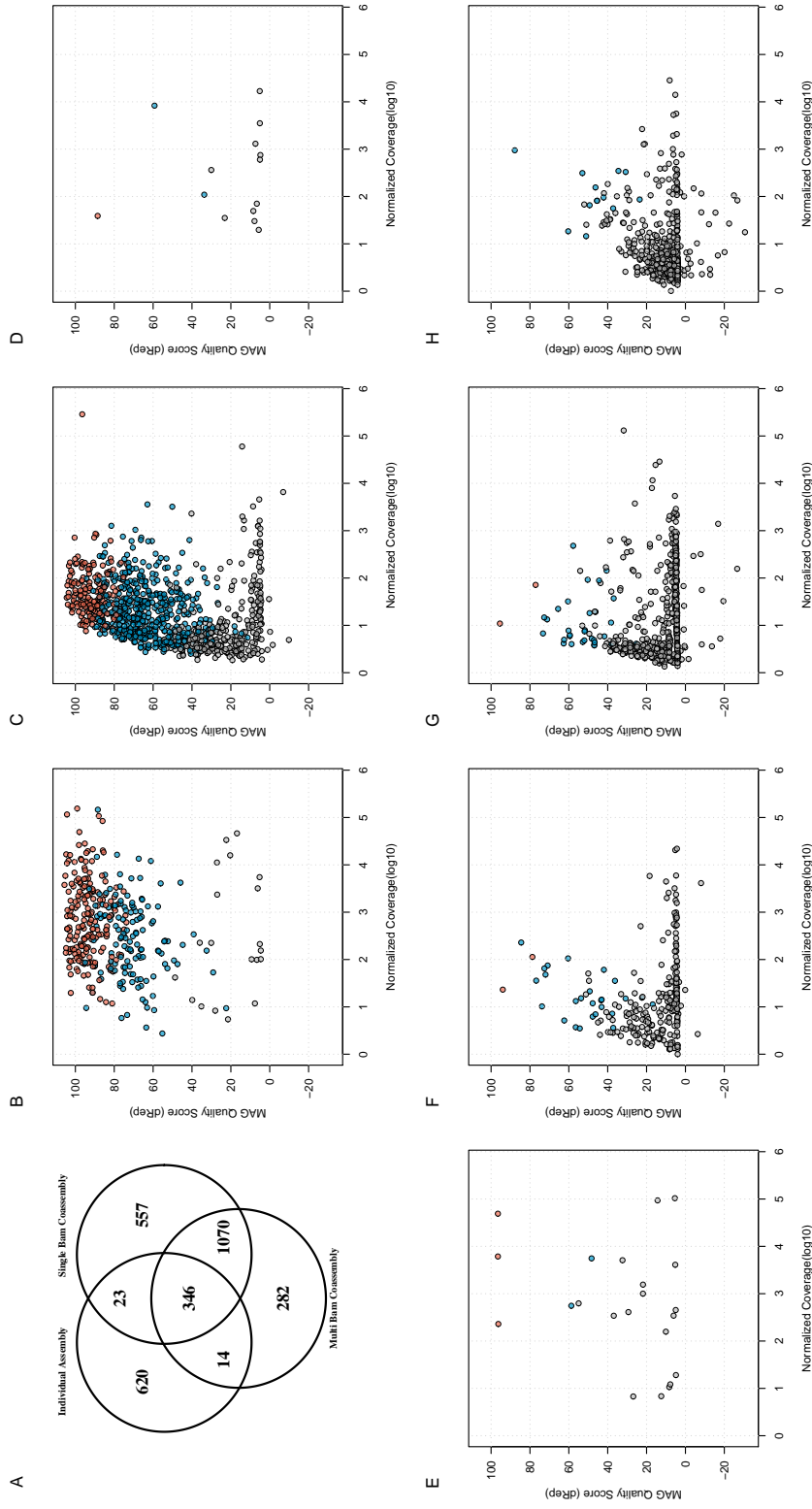


Figure 1: Relationship between genome quality and relative abundance within the MetaBAT2-derived MAG catalogues obtained in this study. Relative abundance is inferred using a normalised measure of coverage, permitting comparison of mean MAG coverage among the three different assembly-binning workflows (see Table 1 and Methods: Genome recovery from individual sample assemblies). Within each decile of the normalised coverage distribution, the numbers of MAG meeting each of the four MIMAG-derived quality levels is shown.





**Figure 2: Inter-relationships between genome quality, relative abundance and recovery workflow type for 7,138 MAGs recovered from the use of MetaBAT2. A) secondary cluster membership by workflow (7,138 MAG categorised into 2,912 secondary clusters; the remaining panels show the highest observed genome quality with a secondary cluster (vertical axis) against normalised coverage measure (horizontal axis) for secondary clusters B) containing MAGs from all three workflows ( $n=346$ ); C) recovered from both single-BAM and multi-BAM co-assembly workflows ( $n=1070$ ); D) recovered from both individual assemblies and multi-BAM co-assembly ( $n=14$ ); E) recovered from both individual assemblies and single-BAM co-assembly ( $n=23$ ); F-H) recovered solely from multi-BAM co-assembly ( $n=282$ ), single-BAM co-assembly ( $n=557$ ) and individual assemblies ( $n=620$ ), respectively. Secondary clusters containing pHQ, MQ, and LQ MAGs are coloured in red, blue, and grey, respectively.**

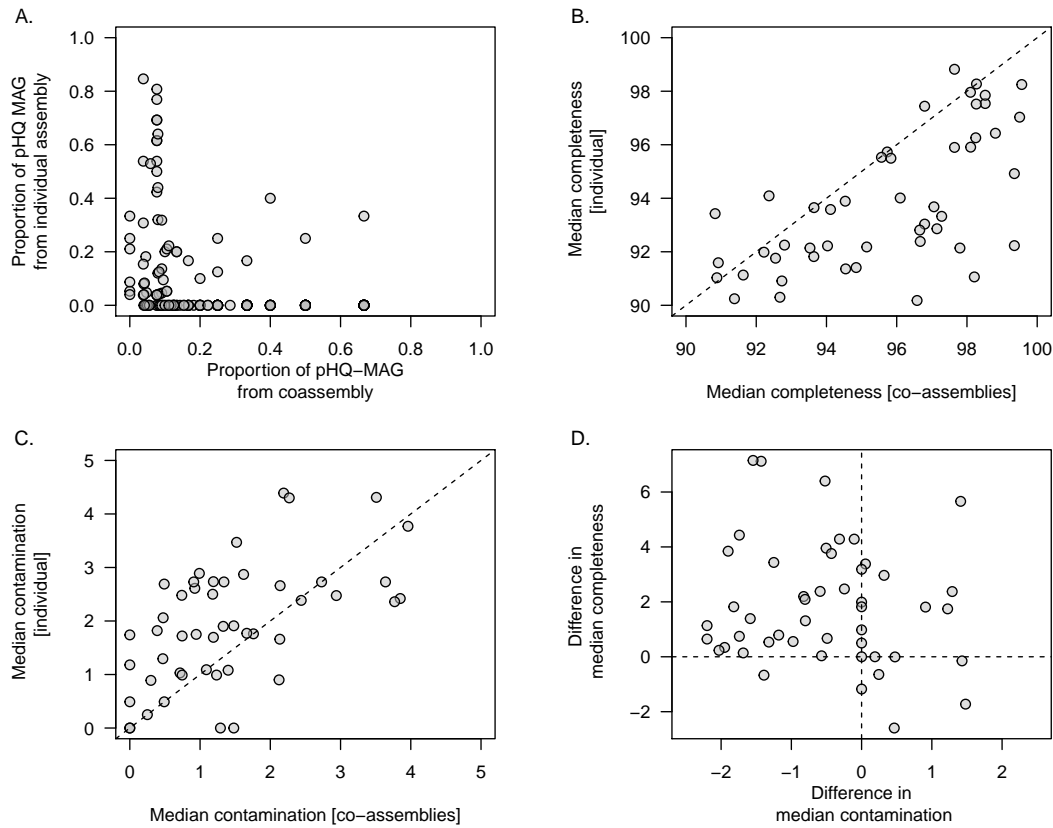


Figure 3: Examination of genome quality in MAGs recovered among different MetaBAT2-derived workflows. Each data point references a secondary cluster of highly related genomes obtained from the dRep workflow. *A*) proportion of MAGs within a secondary cluster that attain pHQ quality status from co-assembly workflows ( $x$ -axis) and individual assemblies ( $y$ -axis); *B–D* comparison of genome quality measures from within 48 secondary clusters in which at least one pHQ MAG is observed from a co-assembly workflow and from an individual assembly; *B*) median completeness ( $C_p$ ) observed from co-assemblies ( $x$ -axis) and individual assemblies ( $y$ -axis); *C*) median contamination ( $C_n$ ) observed from co-assemblies ( $x$ -axis) and individual assemblies ( $y$ -axis); *D*) relationship between the difference in median completeness observed in co-assemblies with respect to individual assemblies ( $y$ -axis) and difference in median contamination (co-assemblies with respect to individual assemblies) ( $x$ -axis).

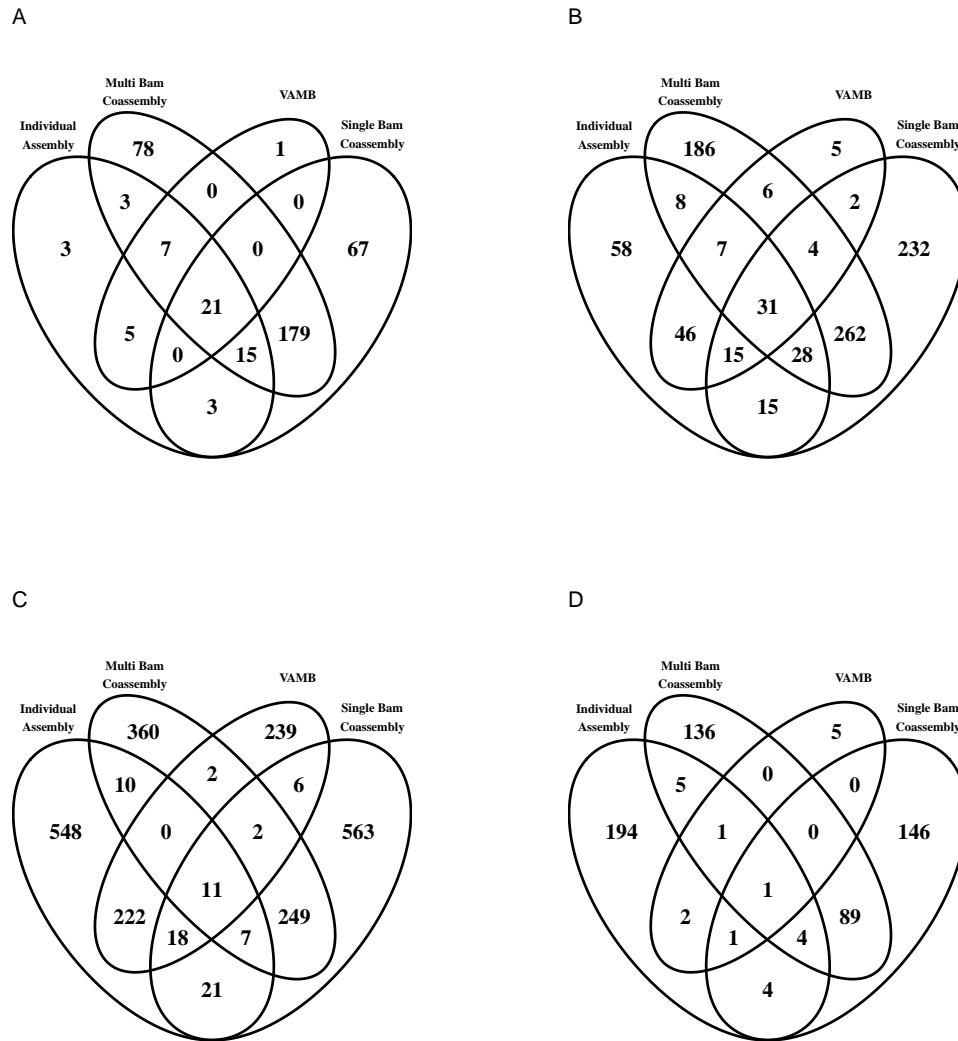


Figure 4: MAG recovery across all four workflows employed in this study, conditioned by genome quality. The entire set of 9,709 MAGs was categorised by genome quality level, and within each quality genome level further categorised by the workflow of origin observed with each secondary cluster. Venn diagrams showing interrelationships are shown here for *A*) pHQ (putative high quality); *B*) MQ (medium quality); *C*) LQ (low quality) and *D*) UC (unclassified).

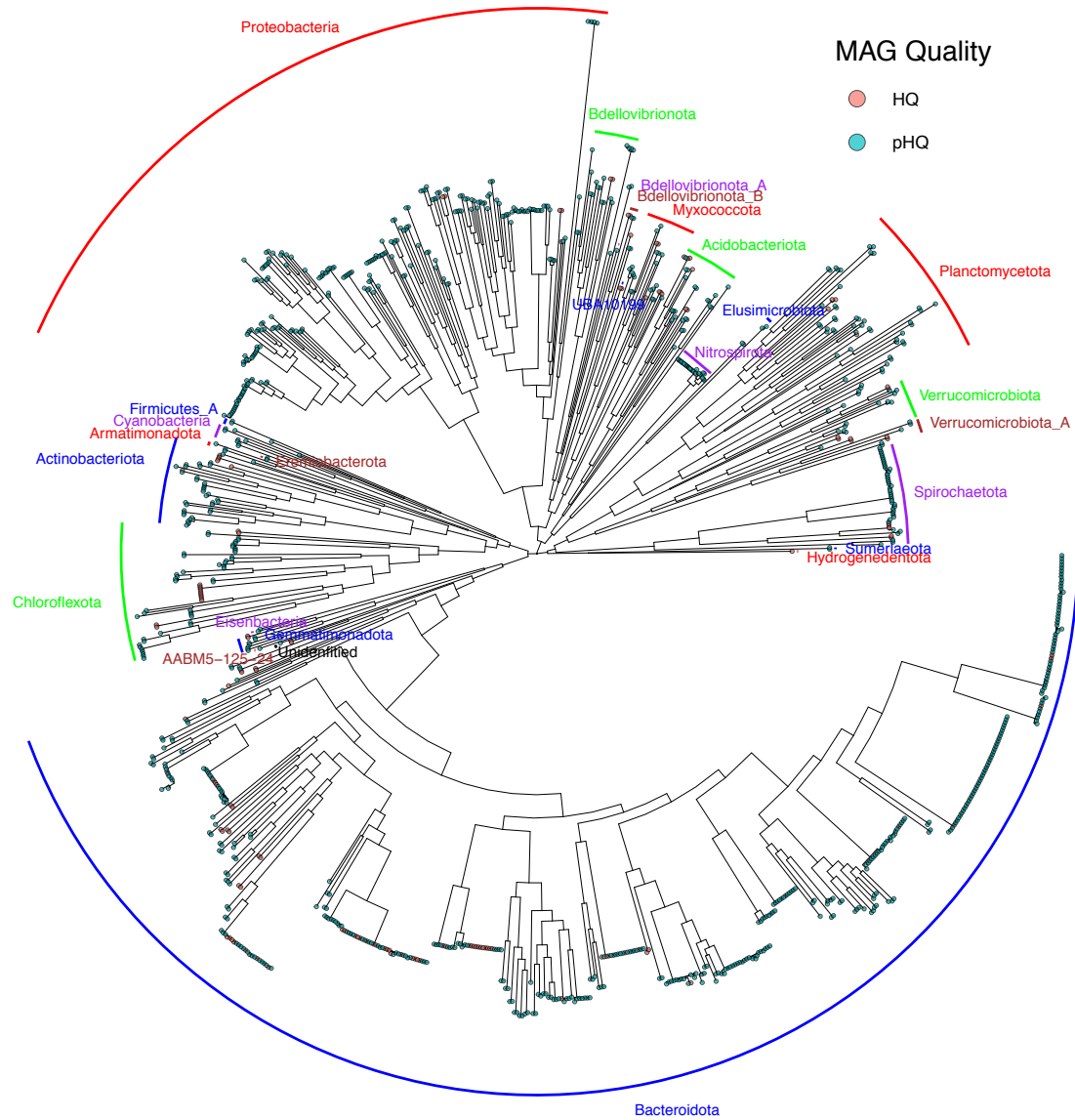


Figure 5: Phylogram of pHQ MAGs recovered from all four workflows used in this study. Phylum level annotations are listed as text labels. MAG holding pHQ status are highlighted in blue-green and the subset of those that hold HQ status under the MIMAG are highlighted in light red.

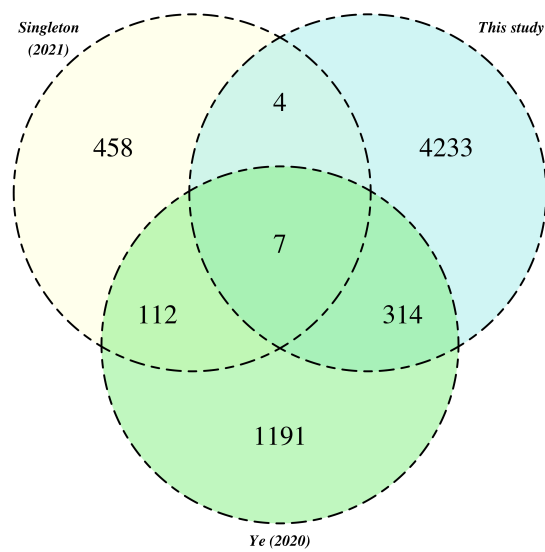


Figure 6: Relationships between pHQ-MAGs recovered in this study and MAGs from extant activated sludge catalogues. Counts reference secondary clusters categorised by the presence of MAGs originating from one of the three MAG catalogues.